JVST Archives 1964-1982
Journal of Vacuum Science & Technology

Computer simulations of resist profiles in xray lithography

K. Heinrich, H. Betz, A. Heuberger, and S. Pongratz

Citation: Journal of Vacuum Science & Technology **19**, 1254 (1981); doi: 10.1116/1.571255
View online: http://dx.doi.org/10.1116/1.571255
View Table of Contents: http://scitation.aip.org/content/avs/journal/jvst/19/4?ver=pdfcov
Published by the AVS: Science & Technology of Materials, Interfaces, and Processing

Computer simulations of resist profiles in x-ray lithography

K. Heinrich, H. Betz, A. Heuberger, and S. Pongratz

Institut für Festkörpertechnologie, Paul-Gerhardt-Allee 42, D-8000 München, West Germany

(Received 15 June 1981; accepted 15 June 1981)

This paper presents a detailed study on computer simulations of resist profiles obtained in x-ray lithography for exposures made either with synchrotron radiation or with an Al–K_α source. It is assumed, for purposes of the calculations, that the vacuum windows consist of kapton and that silicon is used as the mask material. The influence of edge shape and mask absorber thickness upon the resist structure is of special interest. The other parameters affecting resist profiles, such as Fresnel diffraction (especially in the case of semitransparent absorbers) and photoelectron range, are taken into consideration. In the case of the x-ray tube, the penumbral blur caused by the finite dimensions of the source spot leads to an additional deterioration of the edge sharpness. For the calculations, the intensity distribution over the spot area was assumed to be uniform (with Gaussian-shaped edges). The influence of the photoelectron range upon the resist profiles is calculated, using the simple depth-dose relationship of Gruen. The calculated resist profiles are compared with typical experimental results.

PACS numbers: 07.85. + h, 07.68. + m, 41.70. + t, 85.40.Ci

I. INTRODUCTION

The question of the most appropriate x-ray source (the x-ray tube, the synchrotron or, perhaps, a plasma source) has not yet been resolved completely, and in connection with this, the resolution performance of these sources is of special interest and has already been calculated for a special x-ray tube.[1] The plasma sources will not be considered in detail here, because they are in an early stage of development, and the results obtained for the x-ray tube and the synchrotron can easily be applied for plasma as well. The main differences between the alternative sources have to do with the physical dimensions of the source point, the degree of collimation, and the spectral distribution. The monochromatic radiation from an x-ray tube has a high degree of divergence, which leads to the run-out effect, depending on the distance from the middle axis. The finite dimensions of the focus spot cause penumbral blurring. In the case of the electron synchrotron the radiation is strongly collimated and covers a certain spectral range depending on the absorbing media that have to be penetrated. The following calculations are based on the synchrotron radiaton emitted from the electron storage ring "DORIS" at Hamburg. The radiation has its maximum at about 0.8 nm and shows an overall divergence of less than 1 mrad. In the case of the monochromatic x-ray tube we used the Al–K_α radiation with nearly the same wavelength ($\lambda = 0.84$ nm) as the above mentioned maximum of the synchrotron radiation.

II. CONDITIONS FOR THE SIMULATIONS

For simulating the lithography process it is necessary to first calculate the spatial distribution of the deposited radiation energy. We will discuss here the following physical effects:

(1) Fresnel diffraction (especially for semitransparent absorbers), (2) the extension of the focus spot in the case of an x-ray tube, (3) the spectral distribution in the case of the synchrotron exposure, (4) the influence of a beveled absorber edge, and (5) backscattered photoelectrons.

The resist we used was a specially fractionated PMMA with a very high molecular weight. It was possible to ensure that there was no resist removal in the unexposed region. For the actual simulation of the development process we used a simple power law approximation of the measured solubility rate as a function of the absorbed dose. The simulation procedure is a simple step by step algorithm for a chain of points at the momentary resist surface.[2]

A. Fresnel diffraction

In the case of parallel monochromatic radiation (wavelength λ, intensity I_0) and a vertical absorber edge, the classical Fresnel theory leads to the following intensity distribution at the resist:

$$I(x) = \tfrac{1}{2} I_0 \{ [\tfrac{1}{2} + C(w)]^2 + [\tfrac{1}{2} + S(w)]^2 \},$$

where x is the coordinate at the resist surface perpendicular to the absorber edge, S, C are the well-known Fresnel integrals, $w = x(2/\lambda \cdot s)^{1/2}$, and s is the proximity gap.

But the classical theory holds only for a fully opaque absorber. For a semitransparent absorber (with transmitted intensity I_1) the complex radiation amplitudes have to be superimposed. The result is the following complex radiation amplitude:

$$U(x) = \tfrac{1}{2} \begin{pmatrix} A_+ - A_-[C(w) + S(w)] \\ A_-[C(w) - S(w)] \end{pmatrix},$$

where $A_\pm = I_0^{1/2} \pm I_1^{1/2}$.

The intensity distribution is $I(x) = |U(x)|^2$.

In the case of x-ray exposure there is an extended source,

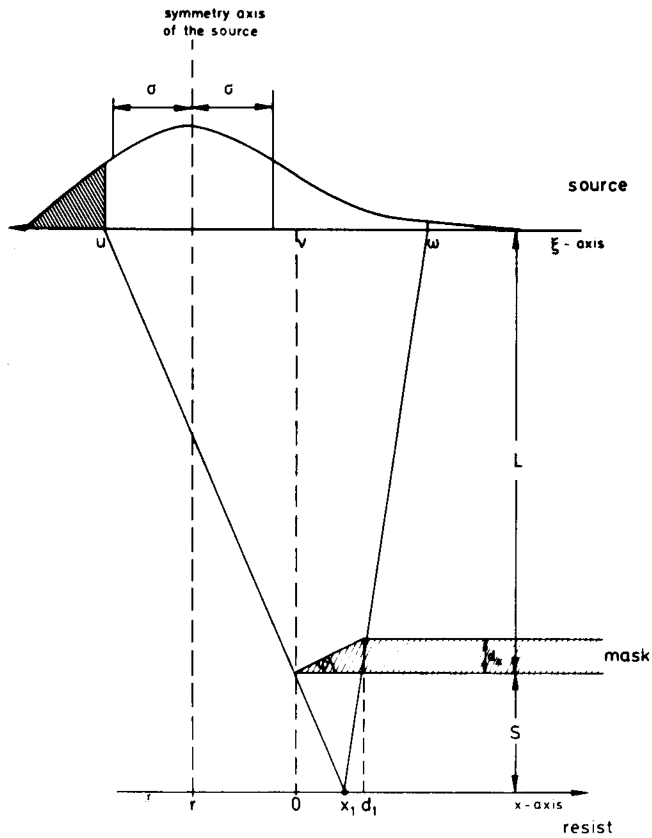

FIG. 1. Schematic of the exposure geometry of a Gaussian-shaped x-ray source and of beveled mask absorber.

and therefore an integration over the source intensity distribution has to be done and the shift due to the central projection has to be considered.

In the case of synchrotron radiation an integration over the spectral distribution has to be done taking into consideration the wavelength dependent absorption.

Figures 2 and 3 show the intensity distribution at the resist calculated for an x-ray tube with different source diameters and for synchrotron radiation at different proximity gaps and absorber thicknesses, respectively.

The power absorbed in the resist at a depth z is

$$P_a(x,z) = \int_{-\infty}^{\infty} I(x,\lambda)\,\alpha_R(\lambda)\exp[-\alpha_R(\lambda)z]d\lambda,$$

where $I(x,\lambda)$ is the wavelength-dependent Fresnel intensity distribution and $\alpha_R(\lambda)$ is the wavelength dependent absorption coefficient of the resist.

The depth dependence of P_a can be approximated by an exponential function

$$P_a(x,z) \approx P(x,0)e^{-\beta(x)z},$$

where

$$\beta(x) = \left[\int \alpha_R^2(\lambda)\,I(x,\lambda)\,d\lambda\right] \Big/ \left[\int \alpha_R(\lambda)\,I(x,\lambda)\,d\lambda\right]$$

B. The beveled absorber edge

Figure 1 shows the schematic of the exposure geometry with a beveled absorber edge and a Gaussian-shaped x-ray source. Different intensity shapes in the focus spot can be approximated by a sum of Gaussian functions. The real intensity shape is nearly rectangular with no abrupt transition to zero at the rim, and was well approximated by 11 Gaussian functions each shifted by $2^{1/2}\sigma$.

For a single Gaussian part of the source shape the absorbed dose at the resist can be easily calculated analytically.

For a point x_1 in the resist plane the source plane is divided into three parts, which correspond to the sections from which the point x_1 obtains radiation through different absorbing regions (see Fig. 1). The total radiation intensity in x_1 is therefore the sum of the following three parts:

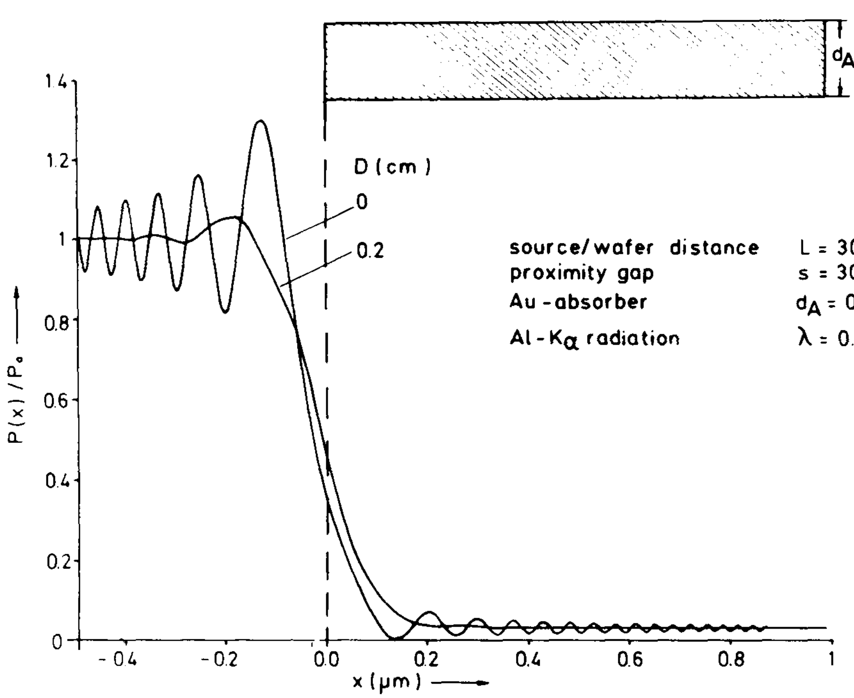

FIG. 2. Influence of focus diameter on the intensity distribution behind a semitransparent gold absorber due to Fresnel diffraction in case of an AL–K_α radiation.

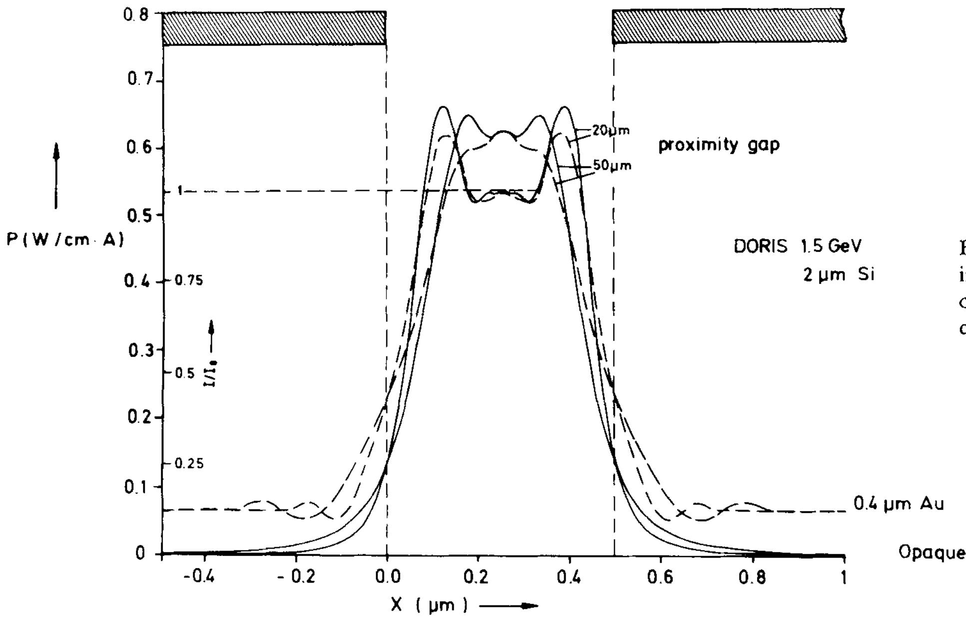

FIG. 3. Fresnel diffraction behind a 0.5 μm slit in case of synchrotron radiation for a fully opaque and a semitransparent absorber with different proximity gaps.

$$I_1 = I_0/2\ \mathrm{erfc}[u/(2^{1/2}\sigma)],$$

$$I_2 = I_0/2\ \exp[-\beta(u-\beta\sigma^2)]\{\mathrm{erfc}[(w-\beta\sigma^2)/(2^{1/2}\sigma)] - \mathrm{erfc}[(u-\beta\sigma^2)/(2^{1/2}\sigma)]\},\ \text{and}$$

$$I_3 = I_0/2\ \exp(-\alpha_A d_A)\mathrm{erfc}[-w/(2^{1/2}\sigma)],$$

where I_0 is the radiation intensity without absorber (for one Gaussian part of the source),

σ is the width of the single Gaussian function,

$\beta = \alpha_A d_A/(u-w)$,

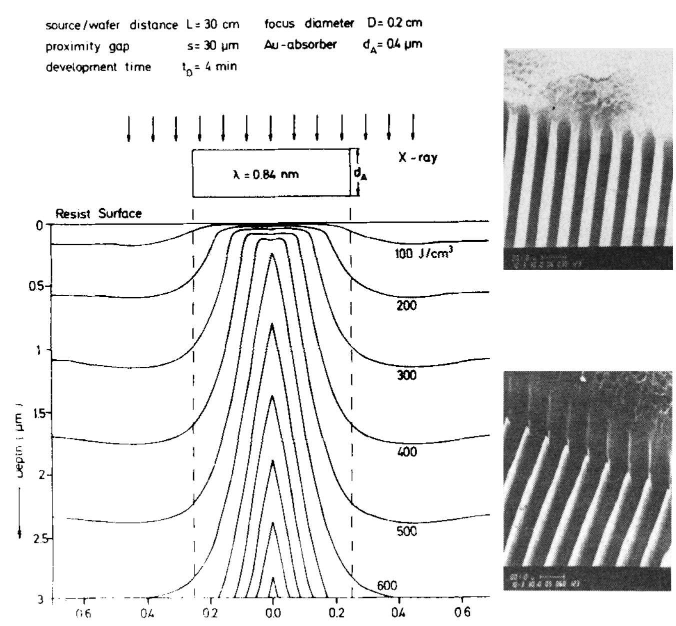

FIG. 4. Resist profiles calculated for x-ray tube exposure, Fresnel diffraction, at different doses (at the resist surface without absorber).

$\alpha_A d_A$ are the absorption coefficient and the thickness of the absorber, respectively,

$u = x_1 L/s - r$,

$w = u - d_A(L/s+1)/\tan\varphi$,

L = source-wafer distance,

s = proximity gap, and

erfc is the complementary error function.

In the case of synchrotron radiation the intensity in a given point x_1 at the resist surface is simply

$$I(x) = \int_0^\infty P(\lambda)\exp[-\alpha_A(\lambda)d(x)]d\lambda,$$

where $P(\lambda)$ is the spectral distribution of synchrotron radiation power and $d(x)$ is the now position-dependent absorber thickness.

C. Photoelectrons

Our approach to calculating the influence of photoelectrons on energy deposition by synchrotron light was to take the usual standard formulas reported in the literature,[3,4] e.g., Gruen's formula, depth dose function, and the angular distribution of direct photoelectrons and Auger electrons.

III. COMPARISON BETWEEN SIMULATIONS AND EXPERIMENTS

Figure 4 shows the computed resist profiles for an exposure with different doses using the Al–K_α radiation. The dose dependence at a fixed development time and the effect of varying development time are qualitatively the same; however, the scaling factor is changed. In this case the effect of Fresnel diffraction using a semitransparent gold absorber of 0.4 μm thickness and with vertical walls has been taken into account. The exposure parameters are the following: source to wafer distance 30 cm, proximity gap 30 μm, and focus diameter 2 mm. The variation of the exposure dose leads from an expanded nearly rectangular resist profile at

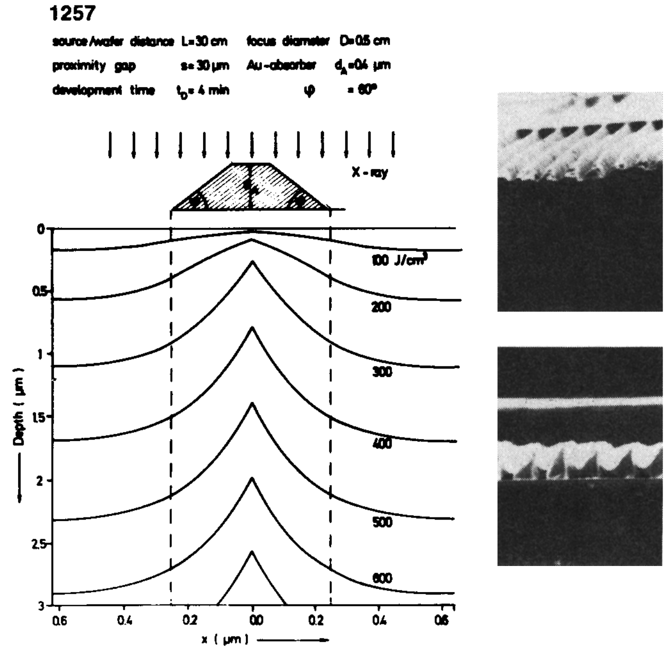

FIG. 5. Resist profiles calculated for x-ray tube exposure, a beveled absorber bar, at different doses.

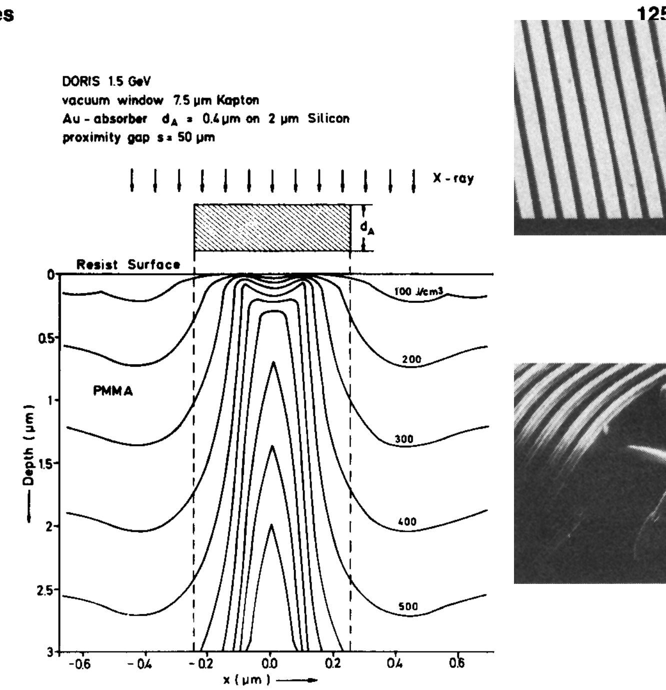

FIG. 7. Resist calculated for synchrotron exposure, Fresnel diffraction, at different doses.

lower doses to a triangle shaped structure at higher ones. The corresponding experimental results are shown on the right side of this figure, where the rectangular but slightly narrowed structures can be seen, which occur at lower doses. The lower SEM picture shows high-dose exposed structures with the related smaller linewidth of only 0.2 μm instead of 0.5 μm and strongly beveled walls.

For the calculation of the profiles shown in Fig. 5, a 60°-beveled absorber (0.4 μm in thickness) was assumed, together with a broad focus spot size of 5 mm. The influence of both factors led to a distortion in the same order of magnitude. The other exposure parameters (source/wafer distance and

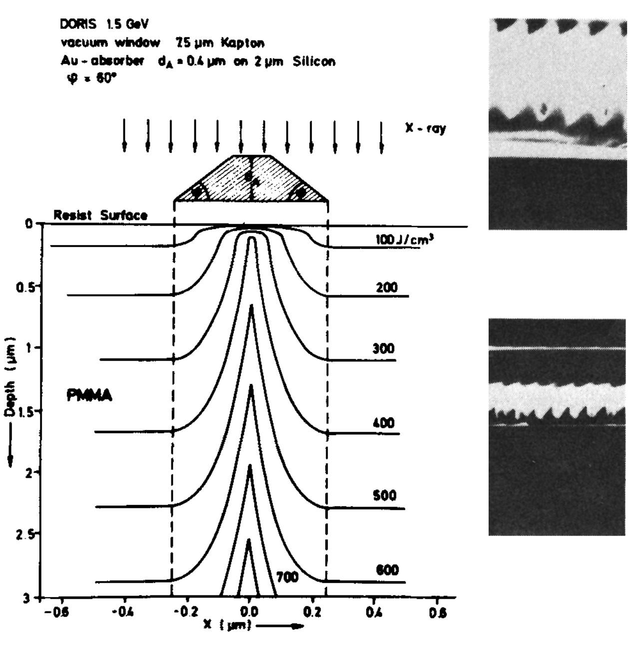

FIG. 6. Resist profiles calculated for synchrotron exposure, a beveled absorber bar, at different doses.

proximity gap) are unchanged compared with the previous figure. The resulting profiles are, of course, much more beveled than in the case of pure Fresnel diffraction. It is nearly impossible, however, to obtain sufficiently steep walls in the high dose region. The related experimental results are given for a 0.5 μm structure exposed to a dose of 300 J/cm^3 in the upper SEM picture. The walls are strongly beveled in shapes even in case of low doses corresponding to the simulation. The high dose (500 J/cm^3) structure, however, shows a little more beveled profile with a remaining resist thickness much smaller than in the upper example (the two bright lines indicate the original resist height).

The simulations shown in Fig. 6 were made for broadband radiation emitted from the electron storage ring DORIS, with the same absorber thickness and bevel as in the previous case. The further exposure parameters are: 7.5 μm kapton window, 2 μm silicon mask. High doses ($\geqslant$ 500 J/cm^3) lead again to triangle shaped profiles with drastically reduced resist thicknesses according to the lower SEM photograph. Employing a lower dose of about 400 J/cm^3, a bell shaped structure as depicted in the upper SEM pictures results.

The exposure parameters of Fig. 7 are the same as in Fig. 6; only the absorber has a vertical edge. The only important parameter is therefore Fresnel diffraction with a semitransparent absorber. Under these circumstances, it is possible to see the influence of Fresnel diffraction clearly. With a dose of around 500 J/cm^3, there is a valley on the top of the structure which can be seen in the corresponding lower SEM picture. The upper picture shows the same structure exposed in contact, in which case no Fresnel effect is to be seen.

Figure 8 takes into account the additional effect of exposure by photoelectrons backscattered from the silicon wafer. These simulations are made for synchrotron radiation using a 60°-beveled gold absorber with a thickness of 0.4 μm. The profile shape is strongly changed near the silicon surface due

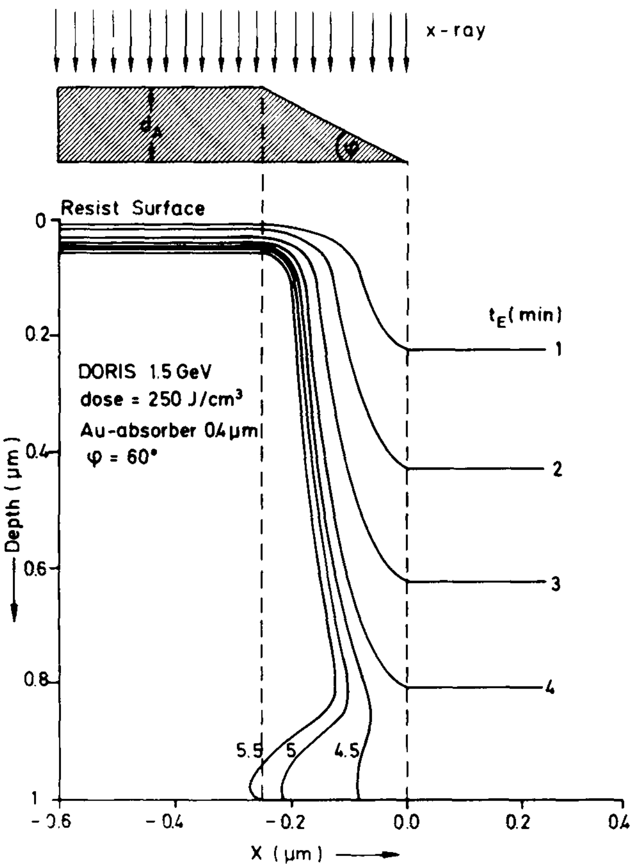

FIG. 8 Resist profiles calculated for synchrotron exposure, a beveled absorber, considering the photoelectron effect, at different development times.

to the influence of the photoelectrons. Although it should be possible to confirm the calculated effect through actual measurements, we could not find any experimental confirmation for these theoretical profiles.

IV. CONCLUSION

In this paper we have presented a detailed study of resist profiles obtained by exposure with an Al–K_α x-ray tube and with synchrotron radiation. The computer simulations have taken into account the finite dimensions of the focus spot, the Fresnel diffraction in the case of semitransparent absorbers, as well as the effect of backscattered photoelectrons.

We found a very good agreement between the computer-simulated and experimental results. Using synchrotron radiation it could be shown that Fresnel diffraction has a measurable effect beneath an absorber being not fully opaque. In the case of an x-ray tube, the replication of 0.5 μm structures seems problematical in thick resists at reasonable proximity distances.

[1] J. R. Maldonado and J. M. Moran, in *Proc. Int. Conf. on Microlithography, Microcircuit Engineering* 80, *Amsterdam*, edited by R. P. Kramer (Delft University, Delft, The Netherlands, 1981).
[2] A. R. Neureuther, J. Vac. Sci. Technol. **15**, 1004 (1978).
[3] P. Tischer and E. Hundt, in *Proc. Electron and Ion Beam Science and Technology*, *8th Int. Conf.*, edited by R. Bakish (Electrochemical Society, Princeton, N. J. 1978).
[4] H. Betz *et al.*, IEEE Trans. Electron Devices **ED-26**, 693–698, (1979).